Nuclear Science and Techniques (2023) 34:127
https://doi.org/10.1007/s41365-023-01267-3

Heuristic techniques for maximum likelihood localization of radioactive sources via a sensor network

Assem Abdelhakim[1]

Received: 22 December 2022 / Revised: 22 April 2023 / Accepted: 5 May 2023 / Published online: 28 August 2023

Abstract
Maximum likelihood estimation (MLE) is an effective method for localizing radioactive sources in a given area. However, it requires an exhaustive search for parameter estimation, which is time-consuming. In this study, heuristic techniques were employed to search for radiation source parameters that provide the maximum likelihood by using a network of sensors. Hence, the time consumption of MLE would be effectively reduced. First, the radiation source was detected using the *k*-sigma method. Subsequently, the MLE was applied for parameter estimation using the readings and positions of the detectors that have detected the radiation source. A comparative study was performed in which the estimation accuracy and time consumption of the MLE were evaluated for traditional methods and heuristic techniques. The traditional MLE was performed via a grid search method using fixed and multiple resolutions. Additionally, four commonly used heuristic algorithms were applied: the firefly algorithm (FFA), particle swarm optimization (PSO), ant colony optimization (ACO), and artificial bee colony (ABC). The experiment was conducted using real data collected by the Low Scatter Irradiator facility at the Savannah River National Laboratory as part of the Intelligent Radiation Sensing System program. The comparative study showed that the estimation time was 3.27 s using fixed resolution MLE and 0.59 s using multi-resolution MLE. The time consumption for the heuristic-based MLE was 0.75, 0.03, 0.02, and 0.059 s for FFA, PSO, ACO, and ABC, respectively. The location estimation error was approximately 0.4 m using either the grid search-based MLE or the heuristic-based MLE. Hence, heuristic-based MLE can provide comparable estimation accuracy through a less time-consuming process than traditional MLE.

Keywords Radioactive source · Maximum likelihood estimation · Multi-resolution MLE · *k*-sigma · Firefly algorithm · Particle swarm optimization · Ant colony optimization · Artificial bee colony

1 Introduction

Radioactive sources are widely used in many nuclear technologies in industry [1], health care [2], nuclear research [3], and isotope production [4]. According to the International Atomic Energy Agency [5], more than 3000 radioactive source incidents have occurred globally, 10% of which were related to trafficking or malicious use. Most applications that use radiation sources are conducted in fixed places, such as hospitals, factories, and laboratories. If radioactive material is lost, a group of technicians searches for the lost source by using handheld detectors. This procedure is time-consuming and may adversely affect the health of the technicians. Hence, developing effective systems for localizing radiation sources in fixed areas is crucial. Distributed sensor networks are commonly used for localization [6, 7]. The network consists of several stationary radiation detectors, in which a radiation source can be localized through a data-processing algorithm using the readings of the detectors.

In this study, localization was performed through a sensor network, where the sensors measured the radiation level and then sent the measured data to a base station. The collected data, including detector readings and positions, were processed to estimate the radiation source parameters. The position of each detector (sensor) is normally provided through a global positioning system receiver [8]. Typically, the radiation source parameters are represented by the source's location and intensity (strength) [9]. In order to perform effective localization, deployed detectors measure gamma-ray radiation, which can travel greater distances than other radiation

✉ Assem Abdelhakim
assem.abdelhakim@eaea.org.eg

[1] Department of Radiation Engineering, National Center for Radiation Research and Technology, Egyptian Atomic Energy Authority, Cairo 11787, Egypt

types. The type of detector used depends primarily on the detection material and the surface area, which affects the detection efficiency [10].

Normally, without the presence of a radiation source, radiation levels can still be detected because of the presence of naturally occurring radioactive materials (NORM) in the surrounding environment [11]. The radiation detected by NORM is referred to as background radiation. Hence, a detection process must be applied before applying the localization method to determine whether the detector reading is due to an anomalous source or NORM. Traditionally, a source is detected if the measured radiation level exceeds a certain value, referred to as the detection threshold. In some sensor networks, data transmission is only performed when a source is detected to reduce the power consumption of each sensor [12]. However, the detection of radiation sources may result in high false positive rates if the background radiation fluctuates significantly according to the concentration of NORM in the surrounding area [13].

The localization of radiation sources is typically applied in environments with uniform background radiation [14] and low variance. Accordingly, background radiation is measured periodically, and the average value of the measured data is used later in the detection or localization process. Many studies have investigated radiation detection and localization while considering different background radiation conditions. For radiation monitoring in large geographic areas, background radiation can be estimated in regions not covered by detectors [15, 16]. In [16], the missing values in the measured radiation data were obtained using the Kriging interpolation method, which is a geo-statistical technique used for predicting spatial attributes. Similarly [15], used the Kriging method to estimate the radiation source parameters and background radiation. Localization using the Kriging interpolation method [15, 16] requires statistical parameters for the predicted data, which may not be available. Furthermore, in Kriging interpolation, an assumption is that the joint probability distribution is fixed in all the studied spaces, which does not hold for all areas. Some methods have been proposed to localize the radiation source in environments with high variance background radiation [13] evaluated using estimation techniques. Usually, estimation methods are used for background radiation and radiation source parameters [13, 17]. However, many observation samples are required for effective estimation [13].

Most of the localization methods are applied in estimating the parameters of unknown radiation sources [18]. However, the source type must be known to perform the localization process accurately. Some methods are used to estimate only the location of the source and can be applied without the knowledge of the source type [19]. In [19], source localization was performed using the ratio of square distances (ROSD), which can only be used to estimate the location parameter. This method provides an accurate estimation using only four sensors in an ideal environment (without any source of randomness). However, more than four sensors are required when background radiation and measurement randomness are considered in practical situations. Localization using ROSD provides many locations where only one location is considered the true location. Accordingly, an additional process is essential to select the true location from the estimated group of locations. Similarly, in [20], the location of the source was estimated using the relationship between the readings of each sensor and the difference between their distances from the source. The intensity of the source was then calculated using the estimated location and average values of the sensor readings. Hence, the accuracy of the estimated intensity depends on the estimated location.

Among the many estimation methods, maximum likelihood estimation (MLE) and Bayesian estimation are commonly applied for radiation source localization [13, 21]. In Bayesian-based estimation methods [18, 21], estimated parameters are assumed to follow a known prior distribution. Hence, the estimation performance relies on the accuracy of the prior distribution, which represents the stochastic process of the source parameters. The authors of [22, 23] and [9] have studied two commonly employed Bayesian estimation methods for localization using particle and Kalman filters, respectively. However, the methods considered are unreliable in practical situations. However, MLE provides reliable estimates without requiring a prior distribution. It is a statistical method that provides the most probable values of the parameters to be estimated according to a likelihood function. MLE has been employed in many radiation-related applications. In [24], background radiation was modeled using MLE via a mobile sensor network for radiation monitoring. In [25], MLE was used to estimate the parameters of multiple radiation sources in a given area where the number of sources is unknown. This method is based on the generalized maximum likelihood rule to estimate the number of sources by exploring different numbers until the best fit with the observation data is achieved. In [13], a localization method for estimating radiation source parameters in an environment with highly fluctuating background radiation was conducted using MLE to localize the source and estimate the background radiation.

Implementing MLE is challenging regarding the radiation localization problem because of the difficulty in finding a closed form solution for the corresponding likelihood function. Normally, MLE is performed numerically through a grid search. This process can be time-consuming, and the duration increases with the size of the search space. Hence, studies have attempted to solve the MLE time consumption problem. Multi-resolution MLE is the most commonly used approach to accelerate the grid search process [11, 26], where the search is performed iteratively. The process is based on decreasing the search boundaries per iteration according to the evaluated estimates provided by the previous iterations. In multi-resolution MLE, the estimation accuracy depends on the initial solution. Accordingly, the search may provide a local maximum rather than a global maximum, referred to as premature convergence.

In this study, we aimed to overcome the time consumption problem of MLE in the localization of radioactive sources. To achieve this objective, we applied alternative search methods using heuristic techniques that reduced the time consumption and likelihood of premature convergence more than multi-resolution MLE has in the literature. According to our review of the literature, heuristic techniques have not been employed for the localization of radiation sources by using MLE. Heuristic methods are inspired by nature, for example, genetic algorithm [27], firefly algorithm [28], particle swarm optimization [29], artificial ant colony [30], artificial bee colony [28], prairie dog optimization [31], gazelle optimization algorithm [32], dwarf mongoose optimization [33], reptile search algorithm [34], and aquila optimizer algorithm [35]. In this comparative study, we investigated the performance of the most commonly used and most effective heuristic methods for solving localization problems. The contributions of this study are as follows:

1. Four common heuristic techniques are used for the maximum likelihood localization of a radiation source, which are: (1) firefly algorithm (FFA), (2) particle swarm optimization (PSO), (3) ant colony optimization (ACO), and (4) artificial bee colony (ABC).
2. The performance of the considered heuristic methods, in terms of estimation error and time consumption, is compared.
3. Verification through experimental results using real data is applied to show that heuristic methods can significantly reduce the time consumption of the MLE localization process.

2 Localization of a radioactive source using MLE

This section describes the localization process in detail. The radiation source parameters, location and intensity, were estimated using the MLE algorithm according to the readings collected from stationary detectors (sensors). For each detector, the gamma-ray radiation was measured in counts per second according to a Poisson distribution model [9] as follows:

$$P\left(R_{i,t} = c_{i,t}\right) = \frac{e^{-\lambda_i}\cdot\left(\lambda_i\right)^{c_{i,t}}}{c_{i,t}!}, 1 \le t \le T_{\mathrm{W}}, \tag{1}$$

where $P(R_{i,t}=c_{i,t})$ is the probability that the reading of the ith detector $R_{i,t}$ at the tth time instant is equal to $c_{i,t}$ counts/s within the measured time window $T_{\mathrm{W}.}$ The reading $R_{i,t}$ depends on the average count rate denoted by λ_i, which can be expressed as follows [36]:

$$\lambda_i = \delta \cdot \frac{I}{{dis_i}^2} + BG, \tag{2}$$

where δ is a constant that depends on the type of radiation isotope and detector parameters, such as the detector area and efficiency. The Euclidean distance between the radiation source and ith detector is referred to as dis_i. The value of BG represents the background radiation emitted from NORM in the environment surrounding the detector. Typically, in localization problems, an assumption is that all the detectors are identical and affected by the same background radiation.

In estimating the radiation source parameters, denoted by Θ, the MLE can be used as follows:

$$\Theta_{\mathrm{ML}} = \left[X_{\mathrm{ML}}, Y_{\mathrm{ML}}, I_{\mathrm{ML}}\right] = \underset{\theta}{\operatorname{argmax}} L(C;\theta), \tag{3}$$

where Θ_{ML} is the estimated parameter that indicates the estimated location (X_{ML}, Y_{ML}) and intensity value I_{ML}. For M detectors, the likelihood function $L(C;\Theta)$ represents the joint probability of the count rates C and the source parameter Θ, where $C=[c_1, c_2, \ldots, c_M]$ is the average count rates of each detector. According to the Poisson model in (1), the likelihood function can be calculated as [13]

$$L(C;\Theta) = \sum_{i=1}^{M}\sum_{t=1}^{T_{\mathrm{W}}}\left(c_{i,t}\cdot \ln\lambda_i - \lambda_i\right). \tag{4}$$

In practice, a detection process must be performed before estimating the radiation source parameters. In other words, all the readings of the M detectors considered in the localization procedure indicate a radiation source in the surrounding area. A simple technique detects a radiation source if the corresponding reading exceeds a threshold value. In this study, the detection threshold value, thr_{d}, was calculated using the k-sigma method as follows:

$$thr_{\mathrm{d}} = \mu_{\mathrm{BG}} + k\cdot\sigma_{\mathrm{BG}}. \tag{5}$$

where μ_{BG} and σ_{BG} are the mean and standard deviation of the readings corresponding to background radiation, respectively. k is a user-defined value that can affect the true-positive rate of detection accuracy. For each detector, the average count rate was calculated and compared with thr_{d} to verify the existence of a radiation source as follows:

$$D_i = \begin{cases} 1 & \text{if } c_i > thr_{\mathrm{d}} \\ 0 & \text{if } c_i \le thr_{\mathrm{d}} \end{cases}, \tag{6}$$

where D_i is a value from the set [0, 1] that indicates the detection status of the ith detector. If D_i is 1, the detector's readings correspond to the radiation source. However, the readings of the ith detector are considered measurements of the background radiation if $D_i = 0$. c_i represents the average count rate measured by the ith detector and is calculated as follows:

$$c_i = \frac{1}{T_W} \sum_{t=1}^{T_W} c_{i,t}. \tag{7}$$

For N detectors deployed in a given area, the k-sigma method was applied periodically to the readings of each detector. All readings collected from the network of detectors are provided in the list R, such as

$$R = [R_1, R_2, \ldots, R_N], \tag{8}$$

where R_i denotes the reading of the ith detector. R_i consists of all readings measured within T_W as follows:

$$R_i = \begin{bmatrix} c_{i,1} \\ \vdots \\ c_{i,T_W} \end{bmatrix}, \tag{9}$$

where $c_{i,t}$ denotes the measured count rate at the tth time instant for the ith detector. If a radiation source is detected by M detectors, where $M \leq N$, the localization algorithm can be performed using the corresponding readings. Figure 1 shows the process of selecting the readings of the detectors that detect a radioactive source according to the k-sigma method. As shown in Fig. 1, the selected readings are stored in a list referred to as *list_R* such that $\|list\_R\| = M$. According to [37], MLE can be applied for radiation source localization using M detectors such that $M \geq 3$.

After selecting the M detectors that detect a radiation source, the corresponding readings in list_R are used for the estimation process using MLE. Due to the nonlinearity relation between the average count rate λ and the source's parameters (X, Y, I), there is no closed form solution to the likelihood function presented in (5). Hence, a search method is used to solve the problem numerically. Search methods were used to find the best solution within the parameters' ranges: [$X_{\min}$, $X_{\max}$], [$Y_{\min}$, $Y_{\max}$], and [$I_{\min}$, $I_{\max}$]. The traditional search method is a midpoint grid search [13], where the range of each parameter is divided into grids of equal size, and the midpoint of each grid is explored. Algorithm 1 presents the MLE algorithm using a midpoint grid search. As shown in Algorithm 1, the parameters' ranges, [$X_{\min}$, $X_{\max}$], [$Y_{\min}$, $Y_{\max}$], and [$I_{\min}$, $I_{\max}$], were divided into N_X, N_Y, and N_I grids, respectively. Hence, the total number of points explored was $N_X \times N_Y \times N_I$. Usually, an equal number of grids is used for each range, that is, $N_X = N_Y = N_I$.

In this study, computational complexity is defined as the number of times the likelihood function (L) is calculated.

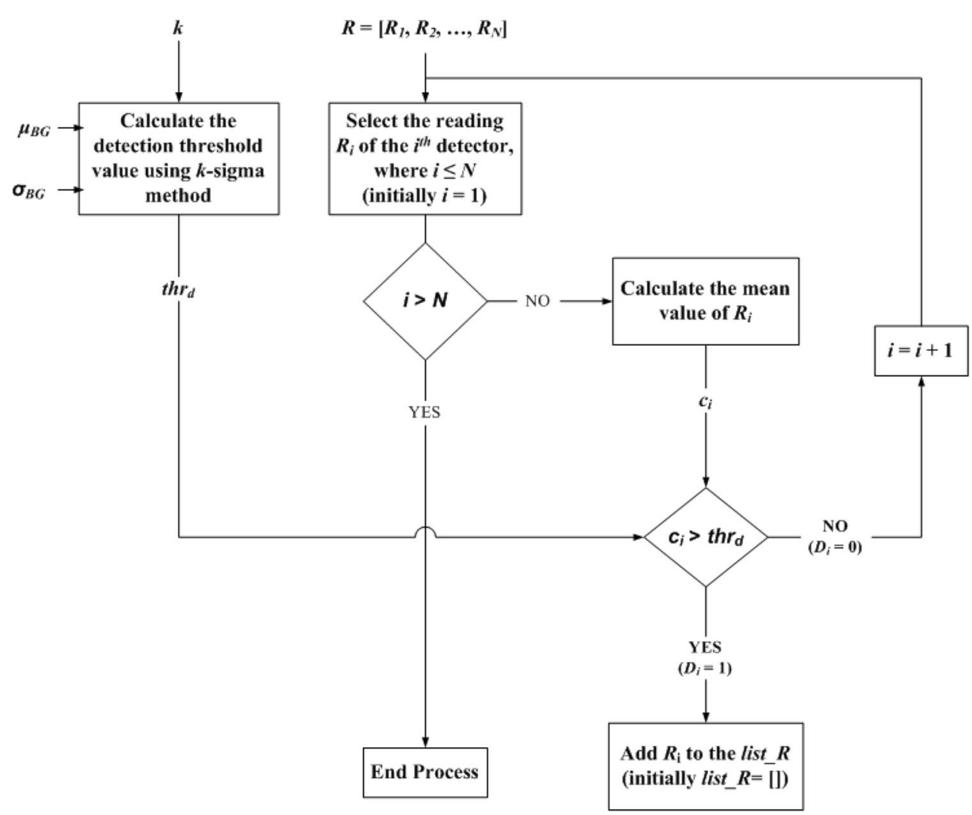

Fig. 1 Process of selecting the readings of the detectors that detected a radiation source

Accordingly, the computational complexity of the MLE using grid search can be provided in terms of the big O notation $O(N_g^3)$, where $N_g = N_X = N_Y = N_I$. Notably, localization accuracy is affected by the number of grids such that better estimates can be obtained using a larger number of grids. However, the time consumption increases as the number of grids increases. The estimation time of the grid search-based MLE, denoted as T_{MLE}, can be calculated according to the following relation:

$$T_{\text{MLE}} = N_g^3 \cdot T_L, \tag{10}$$

where T_L is the time for calculating the likelihood function (L).

Algorithm 1. Midpoint grid search MLE

Inputs:

- Count rate reading $c_{i,t}$ of each detector, where $1 \leq i \leq M$ and $1 \leq t \leq T_W$
- Location (x_i, y_i) of each detector, where $1 \leq i \leq M$.
- Background radiation BG in counts per second (cps)
- Number of points (grids): N_X, N_Y, and N_I
- Parameter range: $[X_{\min}, X_{\max}]$, $[Y_{\min}, Y_{\max}]$, and $[I_{\min}, I_{\max}]$

Procedure**:** Searching for X_{ML}, Y_{ML}, and I_{ML} that maximizes the likelihood L

1. Initialize the likelihood $L_{\max}$ by an arbitrary low value (i.e., $L_{\max} = 0$)
2. For $m = 1 : N_X$
3. For n $= 1 : N_Y$
4. For $p = 1 : N_I$
5. $X_m = X_{\min} + (m - 0.5)\frac{(X_{\max} - X_{\min})}{N_X}$
6. $Y_n = Y_{\min} + (n - 0.5)\frac{(Y_{\max} - Y_{\min})}{N_Y}$
7. $I_p = I_{\min} + (p - 0.5)\frac{(I_{\max} - I_{\min})}{N_I}$
8. Initialize $\lambda = [\ ]$
9. For $i = 1{:}M$
10. $\lambda_i = \delta \cdot \frac{I_k}{(x_i - X_m)^2 + (y_i - Y_n)^2} + BG$
11. Append the value of λ_i to the list λ
12. end For
13. $L = \sum_{i=1}^{M} \sum_{t=1}^{T_W} \left(c_{i,t} \ln \lambda_i - \lambda_i\right)$ // Calculate the likelihood L
14. if $L > L_{\max}$
15. $L_{\max} = L$
16. $X_{ML} = X_m$
17. $Y_{ML} = Y_n$
18. $I_{ML} = I_p$
19. end if
20. end For
21. end For
22. end For

Output: Maximum likelihood estimates X_{ML}, Y_{ML}, and I_{ML}.

Another search method for MLE is multi-resolution MLE [11, 36, 38], which aims to reduce the time consumed by the grid search. In multi-resolution MLE, the search is performed through an iterative process over a parameter range that decreases per iteration. Algorithm 2 presents an MLE algorithm using a multi-resolution grid search. The algorithm applies the conventional grid search using the number of grids N_{X_MR}, N_{Y_MR}, and N_{I_MR}, where $N_{X\_\mathrm{MR}} \ll N_X$, $N_{Y\_\mathrm{MR}} \ll N_Y$, and $N_{I\_\mathrm{MR}} N_I$, respectively. At each iteration, the resulting estimates X_{ML}, Y_{ML}, and I_{ML} were used to calculate the new ranges $[X_{\min}, X_{\max}]$, $[Y_{\min}, Y_{\max}]$, and $[I_{\min}, I_{\max}]$, respectively, to evaluate the new estimated values using Algorithm 1. A significant time reduction can be achieved using multi-resolution MLE without significantly reducing the estimation accuracy compared with traditional grid search MLE. The computational complexity of the multi-resolution MLE can be represented by $O(N^3_{\mathrm{g\_MR}} \cdot N_{\mathrm{itr\_MR}})$ for $N_{\mathrm{g\_MR}} = N_{\mathrm{X\_MR}} = N_{\mathrm{Y\_MR}} = N_{\mathrm{I\_MR}}$, where $N_{\mathrm{itr\_MR}}$ is the number of iterations. Accordingly, the estimation time of the multi-resolution grid search MLE can be formulated as.

$$T_{\mathrm{MR\_MLE}} \approx N^3_{\mathrm{g_{MR}}} \cdot N_{\mathrm{itr_{MR}}} \cdot T_L, \tag{11}$$

where $T_{\mathrm{MR\_MLE}}$ is the time consumed by the MLE using a multi-resolution grid search. One limitation of the multi-resolution MLE is that the search method can provide a local maximum solution rather than the global maximum. In other words, the algorithm does not present a procedure for avoiding convergence toward a local maximum solution in the search space.

Algorithm 2. Multi-resolution grid search MLE

Inputs:

- Readings $c_{i,t}$ of each detector, where $1 \le i \le M$ and $1 \le t \le T_W$
- Location (x_i, y_i) of each detector, where $1 \le i \le M$.
- Background radiation BG in counts per second (cps)
- Number of points: N_{X_MR}, N_{Y_MR}, and N_{I_MR}
- Number of iterations, N_{itr_MR}
- Initial values for parameter ranges $[X_{\min}, X_{\max}]$, $[Y_{\min}, Y_{\max}]$, and $[I_{\min}, I_{\max}]$

Procedure: Searching for the X_{ML}, Y_{ML}, and I_{ML} that maximizes the likelihood L

1. Apply Algorithm 1 to find X_{ML}, Y_{ML}, and I_{ML} by using the initial parameter range and the new number of points N_{X_MR}, N_{Y_MR}, and N_{I_MR}

2. For $l = 1$: N_{itr_MR}

3. $X_{\min} = X_{ML} - 0.5 \frac{(X_{\max} - X_{\min})}{N_{x\_MR}}$

4. $X_{\max} = X_{ML} + 0.5 \frac{(X_{\max} - X_{\min})}{N_{x\_MR}}$

5. $Y_{\min} = Y_{ML} - 0.5 \frac{(Y_{\max} - Y_{\min})}{N_{y\_MR}}$

6. $Y_{\max} = Y_{ML} + 0.5 \frac{(Y_{\max} - Y_{\min})}{N_{y\_MR}}$

7. $I_{\min} = I_{ML} - 0.5 \frac{(I_{\max} - I_{\min})}{N_{I\_MR}}$

8. $I_{\max} = I_{ML} + 0.5 \frac{(I_{\max} - I_{\min})}{N_{I\_MR}}$

9. Apply Algorithm 1 to find X_{ML}, Y_{ML}, and I_{ML} by using the new ranges

10. end For

Output: The maximum likelihood estimates X_{ML}, Y_{ML}, and I_{ML}.

3 Localization using heuristic-based MLE

Heuristic techniques can be used to reduce search time and guarantee an optimum or near optimum solution. We studied the effect of heuristic methods on the performance of maximum likelihood localization of radioactive sources. Figure 2 presents the basic procedure for MLE using a heuristic-based search applied for estimating the radiation source parameter Θ. As shown in Fig. 2, the optimum solution was selected from a solution space bounded by $\Theta_{\min} = [X_{\min}, Y_{\min}, I_{\min}]$

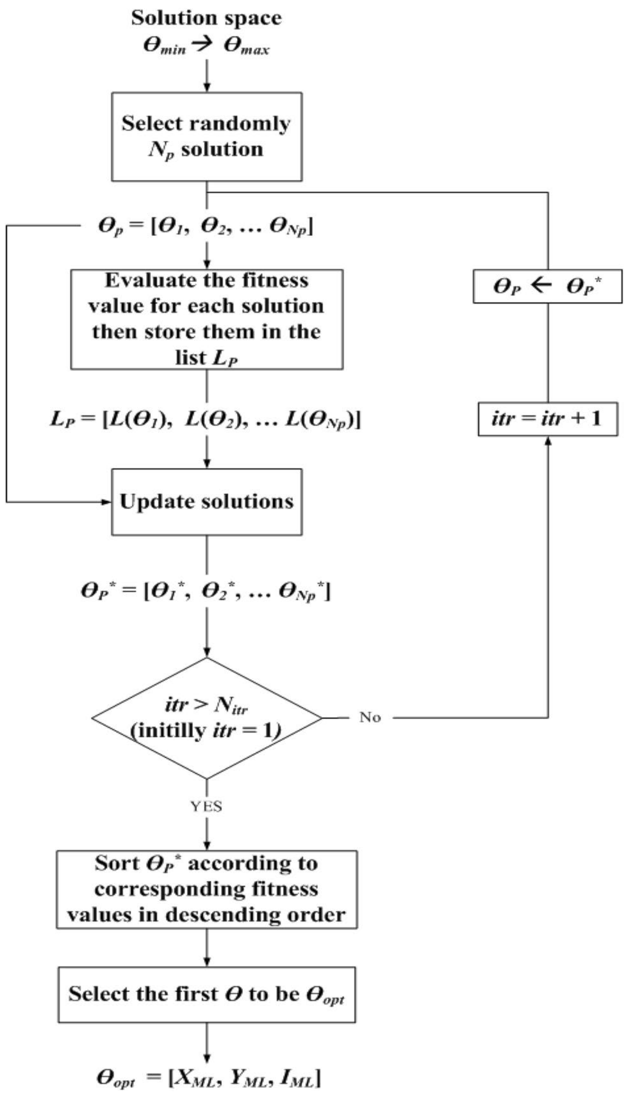

Fig. 2 Heuristic-based search MLE for estimating radiation source parameters X_{ML}, Y_{ML}, and I_{ML}

and $\Theta_{\max} = [X_{\max}, Y_{\max}, I_{\max}]$. Initially, N_{p} solutions are randomly selected to represent the search population as follows:

$$\Theta_{n,d} = \Theta_{\min,\mathrm{d}} + \epsilon \cdot \left(\Theta_{\max,\mathrm{d}} - \Theta_{\min,\mathrm{d}}\right), \quad 1 \le n \le N_{\mathrm{p}}, 1 \le d \le Dim_{\theta}, \tag{12}$$

where $\Theta_{n,d}$ is the dth dimension of the nth solution in the N_{p} solutions, and Dim_{Θ} is the dimension of the parameter Θ. A random selection is conducted using a random value ϵ that follows a uniform distribution over the range [0, 1]. After the initialization step, the N_{p} solutions are stored in the list Θ_{P} as follows:

$$\Theta_{\mathrm{P}} = \left[\Theta_1, \Theta_2, \cdots, \Theta_{N_{\mathrm{p}}}\right]. \tag{13}$$

Each parameter (solution) Θ_n was evaluated using the likelihood function $L(\Theta_n)$ that represents the fitness function, where $1 \le n \le N_{\mathrm{p}}$. The search was then performed in a stochastic manner through an iterative process such that solutions with high fitness values could be found. In the heuristic method, a solution update technique is used to generate new solutions from randomly selected solutions. Hence, each heuristic method has a different computational complexity. In the next subsections, four heuristic methods are presented for the maximum likelihood localization of the radiation sources.

3.1 FFA-based MLE

The FFA is a population-based optimization method [28] that simulates the behavior of fireflies to attract mating partners. It is easily implemented to search for optimal solutions from a continuous range of values. The selection is performed, where a firefly moves toward another firefly that produces the brightest light. For the two fireflies, the observed light intensity (brightness) decreases as the distance between them increases according to the inverse square law. Algorithm 3 presents the pseudo code of the FFA-based MLE used to localize a radiation source. The algorithm simulates the behavior of fireflies to select the maximum likelihood estimates such that.

- The solution space represents the locations of all possible fireflies in a given area.
- The fitness value $L(\Theta_n)$ indicates the light intensity of the nth firefly according to its location represented by the parameter value Θ_n.
- The solution update represents the movement of a firefly at location Θ_n toward another firefly located at Θ_m according to the following relation [39]:

$$\Theta_n^* = \Theta_n + \beta_0 e^{-\gamma \cdot dis_{n,m}^2}\left(\Theta_n - \Theta_m\right) + \alpha\epsilon, 1 \le n \le N_{\mathrm{p}}, \tag{14}$$

where Θ_n^* is the updated value for the nth solution Θ_n. The values of β_0 and γ indicate the attractiveness and the light absorption coefficient, respectively. To prevent a premature convergence toward local optima, the term $\alpha\epsilon$ is added for further randomization. Parameter α is referred to as the randomization parameter. The distance between Θ_n and Θ_m is denoted by $dis_{n,m}$, which is calculated as follows:

$$dis_{n,m} = \sqrt{\sum_{d=1}^{D_{\Theta}} \left(\Theta_{n,d} - \Theta_{m,d}\right)^2}, \tag{15}$$

where $\Theta_{n,d}$ and $\Theta_{m,d}$ are the values of the dth dimension of Θ_n and Θ_m, respectively.

- The optimum solution represents the location of the firefly with the highest brightness.

According to the pseudo code in Algorithm 3, the computational complexity of the FFA-based MLE can be expressed as $O(N_p^{\ 2}\ N_{itr})$. Hence, the estimation time for FFA-based MLE can be calculated as follows:

$$T_{FFA\_MLE} \approx N_p^2 \cdot N_{itr} \cdot T_L, \tag{16}$$

where T_{FFA_MLE} is the time required by the MLE algorithm using an FFA-based search.

3.2 PSO-based MLE

In PSO, the search procedure is inspired by the foraging behavior of animals, for example, birds or fish [29]. Each particle represents a location in the search space and has a memory that stores its best location per iteration, referred to as *pbest* (personal best). Similarly, the overall best location of the swarm (population) is stored in memory as the *gbest* (global best). The algorithm defined the swarm, position, and velocity of each particle. Initially, the positions and velocities of the population were randomly evaluated. Next,

Algorithm 3. FFA-based MLE

Inputs:

- Population size N_p
- Number of iterations N_{itr}
- Solution space: $\Theta_{min} = [X_{min}, Y_{min}, I_{min}]$ and $\Theta_{max} = [X_{max}, Y_{max}, I_{max}]$.
- Fitness function (likelihood function) L
- Solution update parameters: β_0, γ, and α

Procedure**:** Searching for the optimum parameter Θ_{opt}

Initialize population $\Theta_N = [\Theta_1,\ \Theta_2, \ldots\ \Theta_{Np}]$
$itr = 1$
While ($itr \le N_{itr}$)
    For $n = 1 : N_p$
        Calculate the likelihood function $L(\Theta_n)$
        For $m = 1 : N_p$
            Calculate the likelihood function $L(\Theta_m)$
            if $L(\Theta_n) < L(\Theta_m)$ // (update solution Θ_n)
                $\theta_n \leftarrow \theta_n + \beta_0\, e^{-\gamma\, dis_{n,m}{}^2}(\theta_n - \theta_m) + \alpha\,\epsilon$
            else // (move randomly)
                $\theta_n \leftarrow \theta_n + \epsilon \cdot (\theta_{max} - \theta_{min})$
            end if
        end For
    end For
    Sort the N_p solutions according to their fitness value in descending order
    $itr = itr + 1$
end While
The first of the sorted N_p solutions is selected as the optimum solution Θ_{opt}.

Output: The maximum likelihood estimate $\Theta_{opt} = [X_{ML}, Y_{ML}, I_{ML}]$.

the position and velocity were updated per iteration according to the values of *pbest* and *gbest* as follows:

$$v_n^* = w \cdot v_n + a_1\epsilon_1\left(pbest_n - x_n\right) + a_2\epsilon_2\left(gbest - x_n\right), \tag{17}$$

$$x_n^* = x_n + v_n^*, \tag{18}$$

where $x_n^{\ *}$ and $v_n^{\ *}$ denote the updated values for the nth position x_n and velocity v_n, respectively. The parameters a_1 and

a_2 are the acceleration constants used to guide the search toward the best local and global locations, respectively. Furthermore, ϵ_1 and ϵ_2 are random variables, and each follows a uniform distribution over the interval [0, 1]. A weight value denoted by w is used to control the exploration and exploitation of the swarm and is referred to as the inertia weight [40]. The values of *pbest* and *gbest* are the positions corresponding to the best fitness values for a single particle and the overall population, respectively. The pseudo code for the PSO-based MLE is presented in Algorithm 4. The particles' positions are represented by the radiation source parameters Θ_{P}, which are initialized according to (13). However, the velocity of each particle is initialized to a small random value according to [41], where r is a small constant value:

$$v_n = r \cdot \epsilon, 1 \le n \le N_{\mathrm{p}}, \tag{19}$$

As shown in Algorithm 4, the computational complexity of PSO-based MLE is $O(N_p\, N_{\mathrm{itr}})$. Accordingly, the time consumption of the PSO-based MLE can be expressed as

$$T_{\mathrm{PSO\_MLE}} \approx N_{\mathrm{p}} \cdot N_{\mathrm{itr}} \cdot T_{\mathrm{L}}, \tag{20}$$

where $T_{\mathrm{PSO\_}MLE}$ is the estimation time of the PSO-based MLE.

Algorithm 4. PSO-based MLE

Inputs:

- Population size N_p
- Number iterations N_{itr}
- Solution space: $\Theta_{\min} = [X_{\min}, Y_{\min}, I_{\min}]$ and $\Theta_{\max} = [X_{\max}, Y_{\max}, I_{\max}]$.
- Fitness function (likelihood function) L
- Solution update parameters: w, c_1, and c_2

Procedure: Searching for the optimum parameter Θ_{opt}

Initialize population: $\Theta_P = [\Theta_1, \Theta_2, \dots \Theta_{Np}]$ and $V_N = [v_1, v_2, \dots, v_{Np}]$
Calculate the likelihood $L_P = [L_1, L_2, \dots, L_{Np}]$, where $L_n = L(\Theta_n)$.
$pbest_n = \Theta_n, \quad 1 \le n \le N_p$
$gbest = \mathrm{argmax}_\Theta (L_P)$ // store Θ of the maximum likelihood in *gbest*
$L_{\max} = \max (L_P)$ // stores the maximum value of L_P in $L_{\max}$
$itr = 1$
While ($itr \le N_{itr}$)
  For $n = 1 : N_p$
    $v_n^* \leftarrow w \cdot v_n + c_1\epsilon_1(pbest_n - x_n) + c_2\epsilon_2(gbest - x_n)$
    $\theta_n^* \leftarrow \theta_n + v_n$
    Calculate likelihood $L(\Theta_n^*)$
    if $L(\Theta_n^*) > L(\Theta_n)$ // update $pbest_n$
      $pbest_n = \Theta_n^*$
      $\Theta_n = \Theta_n^*$
      $L_n = L(\Theta_n^*)$
    end if
    if $L(\Theta_n^*) > L_{\max}$ // update *gbest*
      $gbest = \Theta_n^*$
    end if
  end For
  $itr = itr + 1$
end While
$\Theta_{\mathrm{opt}} = gbest$

Output: The maximum likelihood estimate $\Theta_{\mathrm{opt}} = [X_{ML}, Y_{ML}, I_{ML}]$.

3.3 ACO-based MLE

ACO was first presented by Colorni et al. [30] as an ant system that simulates ant foraging behavior. During food searching, each ant deposits its pheromone on the path it follows to find the food. Consequently, ants select a path according to the amount of pheromones deposited on that path. A path with more pheromones indicates that it was selected by more ants, representing the shortest path to food. The ACO was first used for discrete optimization problems. Many studies have been conducted on the application of ACO to continuous domains [42]. In this study, ACO was applied to estimate the radiation source parameter by using the MLE according to the following representations:

- The solution space ($\Theta_{\min} \rightarrow \Theta_{\max}$) represents all feasible paths for the population of ants.
- The pheromone level of a selected path is represented by its fitness value, which is calculated using the likelihood function L.
- A new path is selected based on the pheromone levels of the explored paths, according to [43], as follows:

$$\Theta_n^* = R_G, R_G \sim N\left(\Theta_{best}, \sigma_{col}\right), 1 \leq n \leq N_p, \tag{21}$$

where R_G is a random number that follows a Gaussian (normal) distribution of mean Θ_{best} and standard deviation σ_{col}. The value of Θ_{best} represents the best explored path in terms of fitness value. σ_{col} is the standard deviation of all explored paths.

The pseudocode for the ACO-based MLE is presented in Algorithm 5. The computation complexity of the ACO-based MLE can be expressed as $O(N_p N_{itr})$. Furthermore, the time consumption of the ACO-based MLE compared with that of the grid-search-based MLE can be formulated as

$$T_{ACO\_MLE} \approx N_p \cdot N_{itr} \cdot T_L, \tag{22}$$

where T_{ACO_MLE} is the estimation time of the ACO-based MLE.

Algorithm 5. ACO-based MLE

Inputs:

- Population size N_p
- Number iterations N_{itr}
- Solution space: $\Theta_{\min} = [X_{\min}, Y_{\min}, I_{\min}]$ and $\Theta_{\max} = [X_{\max}, Y_{\max}, I_{\max}]$.
- Fitness function (likelihood function) L

Procedure: Searching for optimum parameter Θ_{opt}

Initialize population: $\Theta_P = [\Theta_1, \Theta_2, \ldots \Theta_{Np}]$
Calculate the likelihood $L_P = [L_1, L_2, \ldots, L_{Np}]$, where $L_n = L(\Theta_n)$.
$itr = 1$
While ($itr \leq N_{itr}$)
    $\Theta_{best} = \text{argmax}_{\Theta} (L_P)$
    $\sigma_{col} = \text{Std}(\Theta_P)$ // calculate the standard deviation of Θ_N
    For $n = 1 : N_p$
        $\theta_n^* = R_G, \quad R_G \sim N(\theta_{best}, \sigma_{col})$
        Calculate likelihood $L(\Theta_n^*)$
        if $L(\Theta_n^*) > L(\Theta_n)$ // select better path
            $\Theta_n = \Theta_n^*$
            $L_n = L(\Theta_n^*)$
        end if
    end For
    $itr = itr + 1$
end While
$\Theta_{opt} = \Theta_{best}$

Output: The maximum likelihood estimate $\Theta_{opt} = [X_{ML}, Y_{ML}, I_{ML}]$.

3.4 ABC-based MLE

The ABC algorithm is one of the effective nature-inspired optimization techniques. It was introduced by Karaboga, in [44], as a population-based optimization algorithm that simulates the foraging process of a bee swarm. According to [44], bees search for the highest quality food source by dividing the bee swarm into three groups:

1. Employed bees: explore selected food sources.
2. Onlooker bees: select new food sources for employed bees to explore based on the quality of previously explored sources.
3. Scout bees: randomly explore new food sources.

In ABC, the solution space represents all possible food sources for the bee swarm. Notably, the population represents the location of the food sources to be explored. The solution-updating procedure simulated the behavior of the bees through three stages:

1. Employed stage:

Each solution is updated according to the following relation:

$$\Theta_{n,d}{}^{*} = \Theta_{n,d} + \varnothing \cdot \left(\Theta_{n,d} - \Theta_{r,d}\right), 1 \le n, r \le N_{\mathrm{p}}, \tag{23}$$

where $\Theta_{n,d}{}^{*}$ is the updated value for the dth dimension of the nth solution $\Theta_{n,d}$, and $\Theta_{r,d}$ is the value of the dth dimension of the rth solution. For each solution, only the value of the dth dimension is updated such that d is selected randomly from the range $[1, Dim_{\Theta}]$. The rth solution is selected randomly from the range $[1, N_{\mathrm{p}}]$ under the condition that $r \neq n$. The update equation is based on a random value denoted by Φ, which follows a uniform distribution over the range $[-1, 1]$.

2. Onlooker stage:

A group of solutions is selected for further updating based on the selection probability, denoted by P_n, which is calculated as

$$P_n = \frac{L\left(\Theta_{\mathrm{n}}\right)}{\sum_{m=1}^{N_{\mathrm{p}}} L\left(\Theta_{\mathrm{m}}\right)}, 1 \le n \le N_{\mathrm{p}} \tag{24}$$

3. Scout stage:

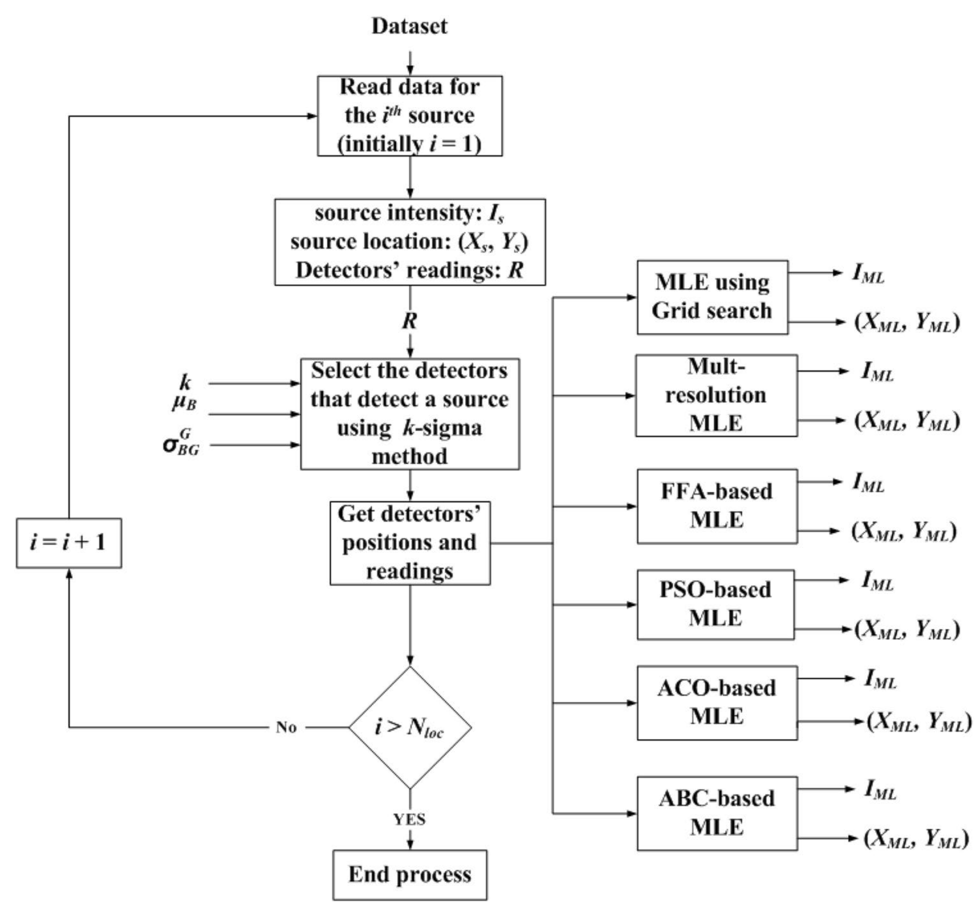

Fig. 3 Procedure for calculating the estimated values

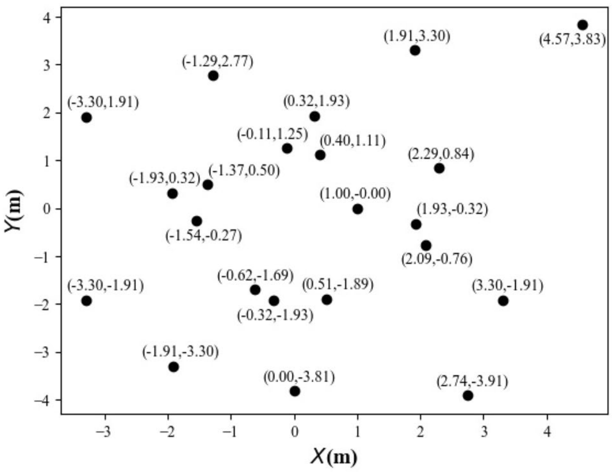

Fig. 4 Locations of radiation detectors inside an area of size 8 m × 8 m, used for collecting the dataset

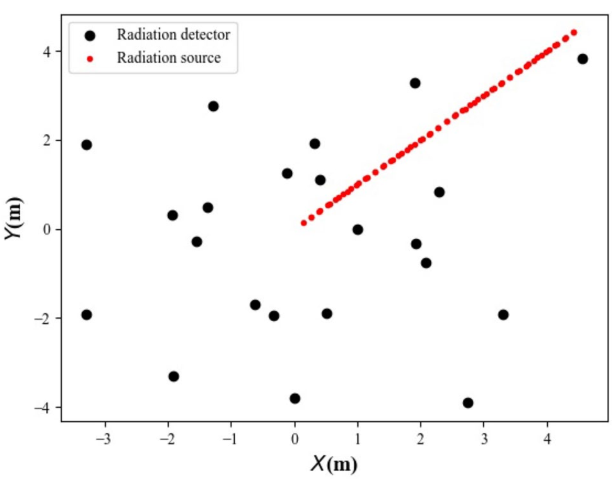

Fig. 5 Considered positions of the radiation source and radiation detectors

In ABC, for each solution, the number of unsuccessful updates (those not providing a better fitness value) is counted and stored in a counter, which is referred to as *trials*. If the value of *trials* exceeds a predefined value, referred to as *Limit*, the solution is randomly updated as follows:

$$\Theta_n^* = \begin{cases} \Theta_{\min} + \epsilon \cdot \left(\Theta_{\max} - \Theta_{\min}\right) & \text{if } trials_n > Limit \\ \Theta_n & \text{Otherwise} \end{cases}, 1 \le n \le N_\mathrm{p}, \tag{25}$$

where $trials_n$ is the value of *trials* for the *n*th solution.

Algorithm 6 presents the pseudo code of the ABC-based MLE method. In the onlooker phase, the selection probability is evaluated and compared with *rand*(0,1), which generates a uniformly distributed random value in the interval [0, 1]. Accordingly, a solution is selected for updating. The onlooker phase is conducted to provide N_p solutions for exploration. Hence, an iterative process is applied until N_p solutions are selected. A number referred to as $N_{\mathrm{max\_look}}$ is defined to limit the number of onlooker iterations, where $N_\mathrm{p} < N_{\mathrm{max\_look}}$. In other words, the number of onlooker iterations is bounded between the minimum and maximum values, N_p and $N_{\mathrm{max\_look}}$, respectively. However, in the scout phase, updating is performed only for solutions whose corresponding *trials* values exceed the value of *Limit*. Hence, the calculation of the fitness function (likelihood function) is conducted N_L times per iteration, where $2N_\mathrm{p} \le N_\mathrm{L} \le 2N_\mathrm{p} + N_{\mathrm{max\_look}}$. Accordingly, the time consumption of the ABC-based MLE can be calculated as

$$T_{\mathrm{ABC\_MLE}} \approx \left(\sum_{i=1}^{N_{\mathrm{itr}}} N_{\mathrm{L}_i}\right) \cdot T_\mathrm{L}, \tag{26}$$

where $T_{\mathrm{ABC\_MLE}}$ is the estimation time for the ABC-based MLE, and $N\mathrm{L}_i$ is the number of times that the likelihood function is calculated at the *i*th iteration.

Table 1 Parameters' values used to conduct the experiment

Experiment parameter		Value
Data parameters	Area size	8 m × 8 m
	Number of detectors (N)	22
	Type of detectors	NaI (Sodium iodide) detector
	Radiation source type	Cesium-137 (^{137}Cs)
	Source's intensity (I)	7.6 μCi and 16 μCi
	Measuring time window (T_W)	6 s
	Number of source locations (N_{loc})	65
PC specifications	CPU type	Intel core-i7
	CPU frequency	2 GHz
	RAM size	16 GB
Programming language specifications	Type	Python
	Version	3.9

Algorithm 6. ABC-based MLE

Inputs:

- Population size: N_{p}
- Number of iterations: N_{itr}
- Maximum number of iterations for the onlooker phase: $N_{\text{max\_look}}$
- Value of *trials*
- Maximum value for *trials*: *Limit*
- Solution space: $\Theta_{\min} = [X_{\min}, Y_{\min}, I_{\min}]$ and $\Theta_{\max} = [X_{\max}, Y_{\max}, I_{\max}]$.
- Fitness function (likelihood function) L

Procedure: Searching for the optimum parameter Θ_{opt}

Initialize population: $\Theta_{\text{P}} = [\Theta_1, \Theta_2, \ldots \Theta_{Np}]$ and $tirals_n = 0$ for $1 \le n \le N_{\text{p}}$
Calculate the likelihood $L_{\text{P}} = [L_1, L_2, \ldots, L_{N\text{p}}]$, where $L_n = L(\Theta_n)$.
$itr = 1$
While ($itr \le N_{\text{itr}}$)
    For $n = 1 : N_{\text{p}}$ // Employed phase
      $d = random\_select\,(1, Dim_\Theta)$ // random selection from the range [1, Dim_Θ]
      $r = random\_select\,(1, N_{\text{p}})$ // such that $r \neq n$
      $\Theta_n^* = \Theta_n$
      $\theta_{n,d}^* = \theta_{n,d} + \emptyset \cdot (\theta_{n,d} - \theta_{r,d})$ // update n^{th} solution
      Calculate likelihood $L(\Theta_n^*)$
      if $L(\Theta_n^*) > L(\Theta_n)$ // select better food source
        $\Theta_n = \Theta_n^*$
        $L_n = L(\Theta_n^*)$
        $trials_n = 0$
      else
        $trials_n = trials_n + 1$
      end if
    end For
    $Count = 1$
    $n = 0$
    $itr_{\text{look}} = 1$
    While ($count \le N_p$) AND ($itr_{\text{look}} \le N_{\text{max\_look}}$) // Onlooker phase.
      $n = n+1$
      if $n > N_{\text{p}}$
        $n = 1$
      end if
      $P_n = \frac{\text{L}_n}{\sum_{m=1}^{Nemp} \text{L}_m}$
      if $P_n > rand(0,1)$ // select Θ_n to be updated
        $d = random\_select\,(1, Dim_\Theta)$
        $r = random\_select\,(1, N_{emp})$
        $\Theta_n^* = \Theta_n$
        $\theta_{n,d}^* = \theta_{n,d} + \emptyset \cdot (\theta_{n,d} - \theta_{r,d})$ // update n^{th} solution
        Calculate likelihood $L(\Theta_n^*)$
        if $L(\Theta_n^*) > L(\Theta_n)$ // select better food source
          $\Theta_n = \Theta_n^*$
          $L_n = L(\Theta_n^*)$
          $trials_n = 0$
        else
          $trials_n = trials_n + 1$
        end if
        $Count = count + 1$
      end if
      $itr_{\text{look}} = itr_{\text{look}} + 1$
    end While
    For $n = 1$: N_{p} // Scout phase
      if $trials_n > Limit$
        $\theta_n^* = \theta_{\min} + \epsilon \cdot (\theta_{\max} - \theta_{\min})$
        Calculate likelihood $L(\Theta_n^*)$
        $\Theta_n = \Theta_n^*$
        $L_n = L(\Theta_n^*)$
      end if
    end For
    Sort the N_{p} solutions according to their likelihood in descending order
    $itr = itr + 1$
end While
$\Theta_{\text{opt}} = \Theta_1$ // Select the first solution to be the optimum solution

Output: The maximum likelihood estimate $\Theta_{\text{opt}} = [X_{\text{ML}}, Y_{\text{ML}}, I_{\text{ML}}]$.

In the next section, we discuss the performance of each search method. Figure 3 shows the procedure performed to provide the estimated values for the evaluation. Each source parameter was read from a given dataset that consists of detector readings from sources at different locations, where the total number of locations is denoted by N_{loc}. The detection process was performed using the k-sigma method, and the estimated parameters were then calculated using the MLE method with different searching techniques.

4 Experimental results

This section presents the performance of the maximum likelihood localization of a radioactive source by using traditional and heuristic search-based methods. In this study, real data were used to evaluate the performance of the MLE methods. The data were collected using the Low Scatter Irradiator facility at the Savannah River National Laboratory as part of the Intelligent Radiation Sensing System program [45, 46]. The count rate measurements were read using 22 stationary radiation detectors scattered in a room with an area of 8 m × 8 m (Fig. 4). First, the detector readings were collected without a radiation source inside the room to measure the background radiation. For the evaluation of the detection and localization methods, radiation sources were placed at different locations inside the room (Fig. 5). The experimental results were calculated using Python 3.9 on a core-i7 PC of 2 GHz and 16 GB RAM. The Python programming language was used for the following: (1) reading the data from the dataset text file, (2) implementing all considered methods, and (3) evaluating the performance of each method. Table 1 lists the experimental parameters.

In this study, we have presented a performance comparison among four heuristic-based search techniques and traditional grid search-based methods applied to MLE. The comparison was conducted in terms of the most significant factors that affect MLE performance: estimation accuracy and time consumption. First, radiation source detection was applied through the k-sigma method using $\mu_{\text{BG}} = 2.4$ cps and $\sigma_{\text{BG}} = 1.5$ cps, calculated from the radiation background dataset. Traditionally, the value of k has been set to 1.645 to control the false positive rate to 5% [47]. Consequently, the detection threshold thr_{d} was 5.4 cps. In the localization process, the likelihood function was evaluated according to the detectors' readings and the average count rate λ by using $\delta = 1.6\ \text{s}^{-1}\ \text{m}^2/\mu\text{Ci}$, calculated via calibration [19]. Notably, the background radiation count rate BG was set to its average value μ_{BG}. Table 2 presents the values of the parameters used for the grid search-based MLE and heuristic-based search MLE. As shown in Table 2, various population sizes and numbers of iterations were used to examine their effect on the performance of heuristic-based

Table 2 Values of parameters used for calculating MLE estimates

MLE parameter	Value
Source Intensity range [I_{min}, I_{max}]	[1, 20] µCi
Source location range	
[X_{min}, X_{max}]	[− 5, 5] m
[Y_{min}, Y_{max}]	[− 5, 5] m
Number of MLE grids (N_g)	30
Number of grids for multi-resolution MLE (N_{g_MR})	10
Number of iterations for multi-resolution MLE (N_{itr_MR})	5
Heuristic-based search parameters	
Population size (N_p)	[5, 10, 15, 20]
Number of iterations (N_{itr})	[5, 10, 15, 20]
Solution space	
Θ_{min}	[− 5, − 5, 1]
Θ_{max}	[5, 20]
FFA update parameters	
β_0	1
Γ	[0.01, 0.1, 1, 5, 10, 15,20, 30]
α	[0.1, 0.25, 0.5, 1]
PSO update parameters	
a_1	[0.1, 0.5, 1, 1.5, 2, 2.5, 3, 3.5, 4]
a_2	[0.1, 0.5, 1, 1.5, 2, 2.5, 3, 3.5, 4]
w	0.8
ABC update parameter	
N_{max_look}	40
Limit	[10, 20, 30, 40, 50]

search MLE methods. According to the dataset parameters listed in Table 1, a suitable range for the source intensity and location was determined. The number of grids used for grid search-based MLE and multi-resolution MLE were selected experimentally. Additionally, different values were selected for the parameters of the heuristic techniques (i.e., FFA, PSO, and ABC) to study their effect on localization performance. Some parameters, such as β_0 and w, were set to their most suitable values, according to the literature, for FFA [39] and PSO [48], respectively.

To evaluate localization performance, we measured the estimation error for the radiation source location and intensity. The location error, denoted as err_{loc}, was represented by the Euclidean distance between the estimated and actual source locations as follows:

$$err_{loc} = \frac{\sum_{m=1}^{N_{Loc}} Dis_m}{N_{Loc}}, \tag{27}$$

where Dis_m is the Euclidian distance between the actual and estimated locations of the m^{th} source as follows:

$$Dis_m = \sqrt{\left(X_m - \widehat{X}_m\right)^2 + \left(Y_m - \widehat{Y}_m\right)^2}, \tag{28}$$

where $\left(X_m, Y_m\right)$ and $(\widehat{X}_m, \widehat{Y}_m)$ are the coordinates of the mth actual and estimated source locations, respectively. The intensity error, denoted by err_I, was measured using the normalized root mean square error (NRMSE) between the actual and estimated intensities as follows:

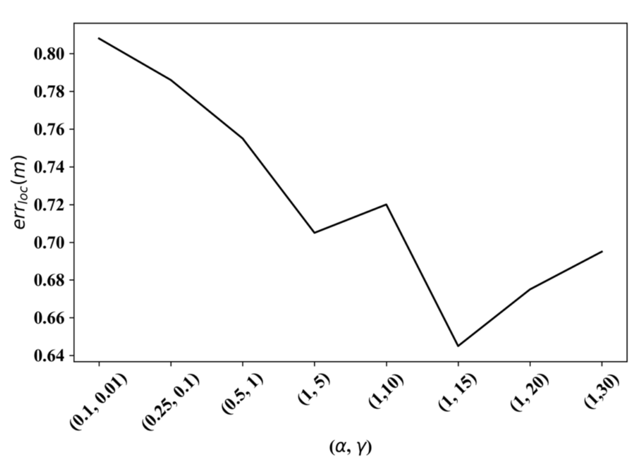

Fig. 6 Location error err_{loc} using FFA-based MLE at different values for parameters α and γ

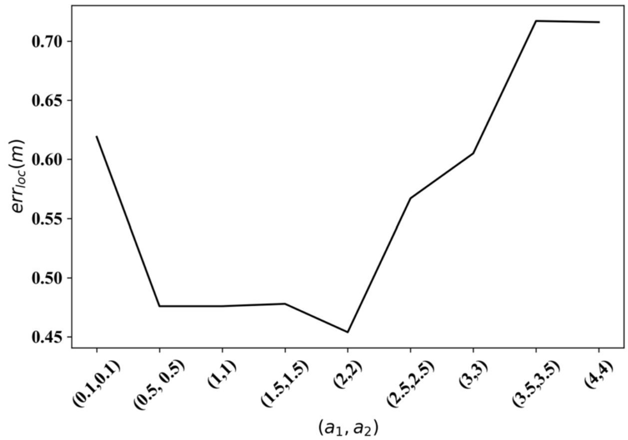

Fig. 7 Location error err_{loc} using PSO-based MLE at different values for parameters a_1 and a_2

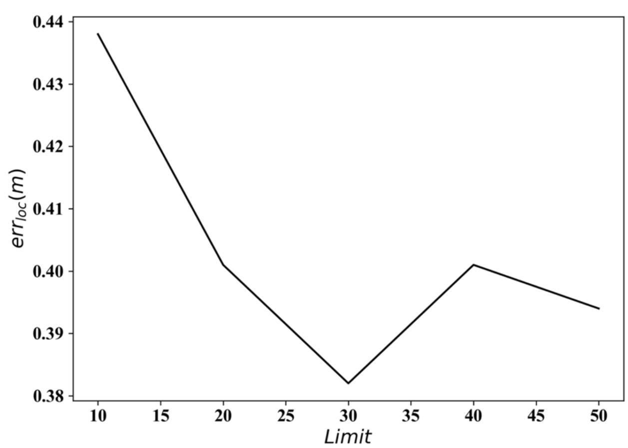

Fig. 8 Location error err_{loc} using ABC-based MLE at different values for the Limit parameter

$$err_{\text{I}} = \frac{1}{(I_{\max} - I_{\min})} \cdot \sqrt{\frac{\sum_{m=1}^{N_{\text{loc}}} \left(I_m - \hat{I}_m\right)^2}{N_{\text{loc}}}}, \tag{29}$$

where I_m and $\hat{I}_m$ are the actual and estimated intensities of the radiation source at the mth location, respectively. The minimum and maximum NRMSE values are 0 and 1, respectively. In evaluating the estimation time, the number of detectors (M) affects the time consumed (t_{L}) for calculating the likelihood function. In the considered experiment, the number of detectors M varied according to the detection threshold thr_{d} and the reading of each detector, such that $3 \le M \le N$. Hence, a different estimation time was provided according to the source's parameters (location and intensity). The average time consumption was used to represent the estimation time for each localization method over the considered source locations and intensities and was calculated as follows:

$$T_{\text{est}} = \frac{1}{N_{\text{Loc}}} \sum_{m=1}^{N_{\text{Loc}}} T_m, \tag{30}$$

where T_{est} is the average estimation time, and T_m is the consumed time to localize the radiation source at the mth location. The time consumed (T_m) by each method was measured using the time module of the Python language.

Usually, in localization problems, the accuracy of the estimated location is considered the most significant factor for performance evaluation [36]. Hence, in this study, heuristic parameters were selected according to their effects on the location error err_{loc}. Figure 6 shows the location error at different values of α and γ for the FFA-based MLE. Notably, the minimum error was achieved at $\alpha = 1$ and $\gamma = 15$. Similarly, for the PSO-based MLE, Fig. 7 presents the location error at different values of parameters a_1 and a_2, where the best performance can be provided at $a_1 = 2$ and $a_2 = 2$. In Fig. 8, the location error was measured for the ABC-based MLE at different values of the user-defined parameter *Limit*. Accordingly, the *Limit* parameter was set to 30 to minimize the errors.

A performance comparison of the heuristic methods was conducted after setting the parameters of each heuristic method to their best values in terms of the achieved location error. Tables 3 and 4 present a comparison between the heuristic-based MLE methods in terms of the location and intensity estimation errors, respectively, for different population sizes and numbers of iterations. As shown in Table 3, the ACO and ABC algorithms provide a more accurate location estimate than the FFA and PSO do. As aforementioned, the accuracy of the estimation increases with the population size. However, the improvement in the estimation accuracy decreases as the population size increase. According to the results, the difference in performance between the FFA-based MLE using $N_{\text{p}} < 10$ and $N_{\text{p}} > 10$ was relatively large. Similarly, the number of iterations affected the estimation accuracy. As shown in Table 3, the difference between ACO and ABC was not significant in terms of the location error for N_{itr} values greater than 10. Furthermore, the estimation accuracy of the FFA-based MLE was approximately the same for N_{itr} greater than 5. Moreover, population size N_{p} and number of iterations N_{itr} had a slight effect on the intensity estimation error (Table 4). The ABC-based MLE has the least estimation error of the heuristic methods for most of the considered population sizes and numbers of iterations.

According to the estimation time, we expected the time consumption of heuristic-based methods to increase as the population size or the number of iterations increased. Table 5 compares the heuristic-based MLE methods in terms of the estimation time (T_{est}) for different population sizes

Table 3 Comparison of heuristic-based MLE methods: location error err_{loc} (m) at different population sizes N_p and number of iterations N_{itr}

N_{itr}	N_p	FFA-based MLE	PSO-based MLE	ACO-based MLE	ABC-based MLE
5	5	1.320	0.736	0.738	0.624
	10	0.789	0.600	0.571	0.480
	15	0.709	0.533	0.533	0.475
	20	0.650	0.553	0.503	0.381
10	5	1.126	0.636	0.567	0.535
	10	0.779	0.581	0.446	0.466
	15	0.626	0.456	0.446	0.395
	20	0.543	0.492	0.418	0.382
15	5	1.105	0.608	0.528	0.442
	10	0.646	0.522	0.427	0.380
	15	0.636	0.493	0.411	0.372
	20	0.569	0.441	0.401	0.374
20	5	1.066	0.534	0.441	0.473
	10	0.776	0.543	0.393	0.384
	15	0.605	0.437	0.415	0.386
	20	0.581	0.440	0.402	0.366

Table 4 Comparison of heuristic-based MLE methods: intensity error err_I at different population sizes N_p and number of iterations N_{itr}

N_{itr}	N_p	FFA-based MLE	PSO-based MLE	ACO-based MLE	ABC-based MLE
5	5	0.189	0.138	0.117	0.192
	10	0.157	0.128	0.120	0.138
	15	0.138	0.123	0.119	0.118
	20	0.127	0.121	0.108	0.105
10	5	0.175	0.146	0.101	0.155
	10	0.155	0.133	0.097	0.104
	15	0.130	0.118	0.126	0.093
	20	0.117	0.133	0.123	0.077
15	5	0.168	0.130	0.113	0.134
	10	0.163	0.119	0.130	0.094
	15	0.129	0.134	0.142	0.093
	20	0.110	0.131	0.138	0.086
20	5	0.154	0.121	0.131	0.107
	10	0.130	0.130	0.132	0.084
	15	0.118	0.141	0.149	0.089
	20	0.132	0.142	0.143	0.095

and numbers of iterations. The time consumption for the FFA-based MLE increased significantly with an increase in population size. Furthermore, as concluded in the previous section, the PSO-based MLE and ACO-based MLE provide approximately the same estimation time, which is less than that of the ABC-based MLE. Accordingly, the FFA-based MLE is the most time-consuming among the considered heuristic-based MLE methods, especially for large population sizes.

To illustrate the effectiveness of the heuristic-based MLE methods, we compared them with traditional grid search-based MLE methods. The performance value, denoted by P_v, was calculated to indicate the overall performance by using the weighted sum approach as follows:

$$P_v = w_i \cdot err_I + w_l \cdot err_{loc} + w_t \cdot T_{est}, \tag{31}$$

where w_i, w_l, and w_t are the weights of the intensity error, location error, and estimation time, respectively. The weights were calculated for normalization as follows:

$$w_i = \frac{1}{\max\left(err_I\right)}, w_l = \frac{1}{\max\left(err_{loc}\right)}, w_t = \frac{1}{\max\left(T_{est}\right)}, \tag{32}$$

where $\max(err_I)$, $\max(err_{loc})$, and $\max(T_{est})$ are the maximum values of the intensity error, location error, and

Table 5 Comparison of heuristic-based MLE methods: estimation time T_{est} (s) at different population sizes N_p and number of iterations N_{itr}

N_{itr}	N_p	FFA-based MLE	PSO-based MLE	ACO-based MLE	ABC-based MLE
5	5	0.086	0.017	0.016	0.034
	10	0.349	0.027	0.031	0.062
	15	0.758	0.041	0.045	0.090
	20	1.299	0.052	0.057	0.121
10	5	0.172	0.026	0.029	0.066
	10	0.656	0.050	0.055	0.122
	15	1.472	0.072	0.079	0.175
	20	2.615	0.094	0.103	0.229
15	5	0.254	0.038	0.042	0.095
	10	0.992	0.072	0.077	0.176
	15	2.238	0.103	0.115	0.259
	20	3.922	0.137	0.149	0.343
20	5	0.334	0.049	0.055	0.125
	10	1.332	0.091	0.103	0.235
	15	2.909	0.137	0.149	0.341
	20	5.187	0.179	0.198	0.465

Table 6 Comparison of heuristic-based MLE methods: performance value P_v at different population sizes and number of iterations

N_{itr}	N_p	FFA-based MLE	PSO-based MLE	ACO-based MLE	ABC-based MLE
5	5	2.013	1.280	1.172	1.481
	10	1.491	1.129	1.062	1.095
	15	1.406	1.055	1.031	0.992
	20	1.422	1.064	0.955	0.857
10	5	1.805	1.247	0.961	1.226
	10	1.536	1.147	0.853	0.918
	15	1.453	0.979	1.009	0.815
	20	1.557	1.088	0.976	0.732
15	5	1.774	1.149	0.998	1.053
	10	1.563	1.035	1.015	0.810
	15	1.598	1.100	1.074	0.811
	20	1.801	1.052	1.048	0.789
20	5	1.705	1.049	1.027	0.942
	10	1.525	1.113	1.005	0.771
	15	1.648	1.101	1.118	0.813
	20	2.127	1.110	1.082	0.848

estimation time, respectively, calculated for the considered population sizes and the number of iterations. Based on these results, weights were calculated such that $w_i = 5.208$, $w_l = 0.757$, and $w_t = 0.713$. Table 6 compares the heuristic-based MLE methods in terms of performance value P_v. The minimum P_v value was 0.732, obtained using the ABC-based MLE method with the population size and number of iterations equal to 20 and 10, respectively. Hence, a performance comparison of the traditional grid search MLE methods and heuristic-based MLE methods using $N_p = 20$ and $N_{itr} = 10$ was presented.

Table 7 shows the estimated parameters (source intensity and location) at some of the considered source positions in the dataset by using the grid search MLE and the heuristic-based MLE methods. Table 8 compares the performance of traditional grid search-based MLE methods and heuristic-based search MLE methods in terms of estimation error, time consumption, and performance value. The results demonstrate that the multi-resolution grid search significantly reduced the time consumption of MLE and provided estimation accuracy approximately equal to that of a fixed resolution grid search. However, heuristic-based MLE methods present different estimation times and accuracies depending on the solution update procedure of each heuristic technique. The FFA-based MLE method consumes more time and provides

Table 7 Comparison of grid search-based MLE methods and heuristic-based MLE methods according to the estimated parameters $(I_{\mathrm{ML}}, X_{\mathrm{ML}}, Y_{\mathrm{ML}})^{\mathrm{T}}$

Source parameters	Grid search-based MLE		Heuristic-based MLE using			
$\begin{pmatrix} I_s \\ X_s \\ Y_s \end{pmatrix}$	Fixed resolution [13]	Multi-resolution [38]	FFA	PSO	ACO	ABC
$\begin{pmatrix} 7.6 \\ -0.1 \\ -0.1 \end{pmatrix}$	$\begin{pmatrix} 8.9 \\ -0.1 \\ -0.1 \end{pmatrix}$	$\begin{pmatrix} 6.6 \\ 0.3 \\ -0.5 \end{pmatrix}$	$\begin{pmatrix} 11.8 \\ 0.6 \\ 0 \end{pmatrix}$	$\begin{pmatrix} 14.5 \\ 0.6 \\ 0.2 \end{pmatrix}$	$\begin{pmatrix} 12.4 \\ 0.9 \\ 0.4 \end{pmatrix}$	$\begin{pmatrix} 9.9 \\ 0.2 \\ 0 \end{pmatrix}$
$\begin{pmatrix} 16 \\ 0.5 \\ 0.5 \end{pmatrix}$	$\begin{pmatrix} 19.6 \\ 0.1 \\ -0.1 \end{pmatrix}$	$\begin{pmatrix} 17.0 \\ 0.3 \\ 0 \end{pmatrix}$	$\begin{pmatrix} 11.1 \\ 0.7 \\ 0.2 \end{pmatrix}$	$\begin{pmatrix} 16.3 \\ 0.3 \\ 0 \end{pmatrix}$	$\begin{pmatrix} 16.9 \\ 0.3 \\ 0.1 \end{pmatrix}$	$\begin{pmatrix} 16.0 \\ 0.2 \\ 0 \end{pmatrix}$
$\begin{pmatrix} 16 \\ 0.9 \\ 0.9 \end{pmatrix}$	$\begin{pmatrix} 15.2 \\ 1.1 \\ 0.8 \end{pmatrix}$	$\begin{pmatrix} 12.3 \\ 0.9 \\ 0.6 \end{pmatrix}$	$\begin{pmatrix} 14.3 \\ 0.6 \\ 0.7 \end{pmatrix}$	$\begin{pmatrix} 13.4 \\ 0.8 \\ 0.5 \end{pmatrix}$	$\begin{pmatrix} 13.9 \\ 1.1 \\ 0.8 \end{pmatrix}$	$\begin{pmatrix} 15.5 \\ 1.0 \\ 0.6 \end{pmatrix}$
$\begin{pmatrix} 16 \\ 1.4 \\ 1.4 \end{pmatrix}$	$\begin{pmatrix} 6.3 \\ 1.1 \\ 1.1 \end{pmatrix}$	$\begin{pmatrix} 7.2 \\ 1.3 \\ 1.5 \end{pmatrix}$	$\begin{pmatrix} 11.7 \\ 0.6 \\ 0.8 \end{pmatrix}$	$\begin{pmatrix} 17.2 \\ 0 \\ 0.4 \end{pmatrix}$	$\begin{pmatrix} 10.5 \\ 0.6 \\ 1.6 \end{pmatrix}$	$\begin{pmatrix} 10.4 \\ 1.2 \\ 1.5 \end{pmatrix}$
$\begin{pmatrix} 16 \\ 1.8 \\ 1.8 \end{pmatrix}$	$\begin{pmatrix} 16.5 \\ 1.8 \\ 1.8 \end{pmatrix}$	$\begin{pmatrix} 16.1 \\ 1.6 \\ 1.7 \end{pmatrix}$	$\begin{pmatrix} 15.4 \\ 2.4 \\ 1.6 \end{pmatrix}$	$\begin{pmatrix} 17.1 \\ 1.6 \\ 1.8 \end{pmatrix}$	$\begin{pmatrix} 18.8 \\ 1.7 \\ 1.8 \end{pmatrix}$	$\begin{pmatrix} 15.0 \\ 1.6 \\ 1.8 \end{pmatrix}$
$\begin{pmatrix} 16 \\ 2.2 \\ 2.2 \end{pmatrix}$	$\begin{pmatrix} 19.0 \\ 2.5 \\ 2.5 \end{pmatrix}$	$\begin{pmatrix} 17.0 \\ 2.4 \\ 2.4 \end{pmatrix}$	$\begin{pmatrix} 15.2 \\ 1.8 \\ 2.8 \end{pmatrix}$	$\begin{pmatrix} 16.7 \\ 2.1 \\ 2.7 \end{pmatrix}$	$\begin{pmatrix} 15.5 \\ 1.6 \\ 2.9 \end{pmatrix}$	$\begin{pmatrix} 15.0 \\ 2.3 \\ 2.4 \end{pmatrix}$
$\begin{pmatrix} 16 \\ 2.7 \\ 2.7 \end{pmatrix}$	$\begin{pmatrix} 17.1 \\ 2.8 \\ 2.8 \end{pmatrix}$	$\begin{pmatrix} 18.0 \\ 2.8 \\ 2.7 \end{pmatrix}$	$\begin{pmatrix} 16.9 \\ 2.6 \\ 3.1 \end{pmatrix}$	$\begin{pmatrix} 16.5 \\ 2.9 \\ 2.8 \end{pmatrix}$	$\begin{pmatrix} 17.8 \\ 2.7 \\ 3.0 \end{pmatrix}$	$\begin{pmatrix} 15.5 \\ 2.5 \\ 2.9 \end{pmatrix}$
$\begin{pmatrix} 16 \\ 3.2 \\ 3.2 \end{pmatrix}$	$\begin{pmatrix} 17.7 \\ 3.1 \\ 3.1 \end{pmatrix}$	$\begin{pmatrix} 19.9 \\ 2.5 \\ 4.5 \end{pmatrix}$	$\begin{pmatrix} 13.8 \\ 2.6 \\ 2.8 \end{pmatrix}$	$\begin{pmatrix} 17.9 \\ 2.9 \\ 3.7 \end{pmatrix}$	$\begin{pmatrix} 17.6 \\ 2.9 \\ 3.4 \end{pmatrix}$	$\begin{pmatrix} 16.3 \\ 2.9 \\ 3.5 \end{pmatrix}$
$\begin{pmatrix} 16 \\ 3.7 \\ 3.7 \end{pmatrix}$	$\begin{pmatrix} 19.6 \\ 3.5 \\ 3.5 \end{pmatrix}$	$\begin{pmatrix} 18.0 \\ 3.4 \\ 3.4 \end{pmatrix}$	$\begin{pmatrix} 14.2 \\ 3.9 \\ 2.8 \end{pmatrix}$	$\begin{pmatrix} 19.4 \\ 4.1 \\ 3.8 \end{pmatrix}$	$\begin{pmatrix} 19.0 \\ 3.5 \\ 3.4 \end{pmatrix}$	$\begin{pmatrix} 16.9 \\ 3.7 \\ 3.2 \end{pmatrix}$
$\begin{pmatrix} 16 \\ 4.1 \\ 4.1 \end{pmatrix}$	$\begin{pmatrix} 17.7 \\ 3.8 \\ 3.5 \end{pmatrix}$	$\begin{pmatrix} 19.9 \\ 3.7 \\ 3.4 \end{pmatrix}$	$\begin{pmatrix} 16.3 \\ 4.0 \\ 3.5 \end{pmatrix}$	$\begin{pmatrix} 18.5 \\ 4.4 \\ 3.6 \end{pmatrix}$	$\begin{pmatrix} 18.2 \\ 3.8 \\ 3.8 \end{pmatrix}$	$\begin{pmatrix} 17.1 \\ 3.8 \\ 3.5 \end{pmatrix}$

Table 8 Comparison of grid search-based MLE methods and heuristic-based MLE methods: location error (err_{loc}), intensity error (err_{I}), time consumption (T_{est}), and performance value (P_{v})

Performance	Grid search-based MLE		Heuristic-based MLE using			
	Fixed resolution [13]	Multi-resolution [38]	FFA	PSO	ACO	ABC
err_{loc} (m)	0.406	0.406	0.543	0.492	0.418	0.382
err_{I}	0.147	0.168	0.117	0.133	0.123	0.077
T_{est} (s)	3.279	0.592	0.753	0.033	0.027	0.059
P_{v}	3.209	1.381	1.557	1.088	0.976	0.732

lower estimation accuracy than the multi-resolution MLE method does. However, other heuristic techniques (i.e., PSO, ACO, and ABC) provide better accuracy than the FFA and lower estimation time than the multi-resolution MLE. The results in Table 8 verify that the PSO and ACO methods require less time than the ABC method does. In addition, better localization accuracy can be achieved using the ABC-based MLE than by using the considered heuristic-based MLE localization methods.

5 Conclusion

In this study, heuristic techniques were investigated for estimating the parameters of a radiation source using MLE. Detection and localization of the radiation source were performed using a sensor network. First, the detection process was conducted using the *k*-sigma method for each radiation detector. Next, the localization of the radiation source was performed using only the readings and positions of the detectors that detected the source. This study considered four effective heuristic techniques that are commonly used: FFA, PSO, ACO, and ABC. A performance comparison was conducted between the heuristic-based MLE and the traditional MLE by using fixed resolution and multi-resolution grid searches. To provide reliable results, we used real data to evaluate the performance of the considered methods in terms of estimation accuracy and time consumption. The evaluation was conducted by estimating 65 different locations of a ^{137}CS radiation source with intensities of 7.6 µCi and 16 µCi, inside an 8 m × 8 m area, using 22 stationary radiation detectors. According to the results, the considered methods were able to estimate the location of the radiation source with an estimation error of approximately 0.4 m. However, the time consumption varies for each search method. The estimation time using fixed and multi-resolution grid search MLE was 3.27 and 0.59 s, respectively. On the other hand, MLE using FFA, PSO, ACO, and ABC provided maximum likelihood estimates of 0.75, 0.03, 0.02, and 0.059 s, respectively. Hence, the results of this study imply that heuristic-based MLE can provide approximately the same estimation accuracy and less estimation time compared to both the fixed and multi-resolution MLE methods. Furthermore, among the heuristic algorithms considered, the most accurate estimates were obtained using the ACO and ABC methods.

Although heuristic-based MLE methods are less time-consuming than conventional MLE methods, they may not be suitable for real-time applications. In further research, machine learning can be utilized to further reduce the time consumption of the MLE-based localization process. Moreover, additional general localization problems can be considered, such as the localization of (1) more than one radiation source, (2) a radiation source in high variance background radiation, (3) a shielded radiation source, and (4) a moving radiation source.

References

1. J. Guizerix, V. Markovic, P. Airey, Radioisotopes and radiation technology in industry. IAEA Bull. **29**(2), 20–24 (1987)
2. S. Jain, Radiation in medical practice & health effects of radiation: rationale, risks, and rewards. J. Family Med. Prim. Care **10**(4), 1520–1524 (2021). https://doi.org/10.4103/jfmpc.jfmpc_2292_20
3. L. Zhou, S.-M. Wang, D.-Q. Fang et al., Recent progress in two-proton radioactivity. Nucl. Sci. Tech. **33**(8), 105 (2022). https://doi.org/10.1007/s41365-022-01091-1
4. B. Li, N. Tang, Y.-H. Zhang et al., Production of p-rich nuclei with Z= 20–25 based on radioactive ion beams. Nucl. Sci. Tech. **33**(5), 55 (2022). https://doi.org/10.1007/s41365-022-01048-4
5. IAEA: Incident and trafficking database (ITDB). https://www.iaea.org/resources/databases/itdb.
6. S. Sen, N.S. Rao, C.Q. Wu et al., Performance analysis of Wald-statistic based network detection methods for radiation sources, in *IEEE 19th International Conference on Information Fusion (FUSION)* (2016).
7. C.Q. Wu, M.L. Berry, K.M. Grieme et al., Network detection of radiation sources using localization-based approaches. IEEE Trans. Ind. Inf. **15**(4), 2308–2320 (2019). https://doi.org/10.1109/TII.2019.2891253
8. R.J. Nemzek, J.S. Dreicer, D.C. Torney et al., Distributed sensor networks for detection of mobile radioactive sources. IEEE Trans. Nucl. Sci. **51**(4), 1693–1700 (2004). https://doi.org/10.1109/NSSMIC.2003.1352153
9. A. Gunatilaka, B. Ristic, R. Gailis, On localisation of a radiological point source. Inf. Decision Control (2007). https://doi.org/10.1109/IDC.2007.374556
10. C.J. Sullivan, Radioactive source localization in urban environments with sensor networks and the Internet of Things, in *2016 IEEE International Conference on Multisensor Fusion and Integration for Intelligent Systems (MFI)* (2016). https://doi.org/10.1109/MFI.2016.7849518
11. J.Y. Hesterman, L. Caucci, M.A. Kupinski et al., Maximum-likelihood estimation with a contracting-grid search algorithm. IEEE Trans. Nucl. Sci. **57**(3), 1077–1084 (2010). https://doi.org/10.1109/TNS.2010.2045898
12. C. Avram, S. Folea, D. Radu et al., *Wireless Radiation Monitoring System* (ECMS, City of Industry, 2017)
13. E.-W. Bai, A. Heifetz, P. Raptis et al., Maximum likelihood localization of radioactive sources against a highly fluctuating background. IEEE Trans. Nucl. Sci. **62**(6), 3274–3282 (2015). https://doi.org/10.1109/TNS.2015.2497327

14. Z. Liu, S. Abbaszadeh, Double Q-learning for radiation source detection. Sensors **19**(4), 960 (2019). https://doi.org/10.3390/s19040960
15. J. Zhao, Z. Zhang, C.J. Sullivan, Identifying anomalous nuclear radioactive sources using Poisson kriging and mobile sensor networks. PLoS ONE **14**(5), e0216131 (2019). https://doi.org/10.1371/journal.pone.0216131
16. A. Reinhart, *An Integrated System for Gamma-Ray Spectral Mapping and Anomaly Detection* (University of Texas, Austin, 2013)
17. I.J. Michaud, K. Schmidt, R.C. Smith et al., A hierarchical Bayesian model for background variation in radiation source localization. Nucl. Instrum. Methods A **1002**, 165288 (2021). https://doi.org/10.1016/j.nima.2021.165288
18. A. Bukartas, R. Finck, J. Wallin et al., A Bayesian method to localize lost gamma sources. Appl. Radiat. Isotopes **145**, 142–147 (2019). https://doi.org/10.1016/j.apradiso.2018.11.008
19. J.-C. Chin, D.K. Yau, N.S. Rao et al., Accurate localization of low-level radioactive source under noise and measurement errors, in *Proceedings of the 6th ACM Conference on Embedded Network Sensor Systems* (2008).
20. J.-C. Chin, N.S. Rao, D.K. Yau et al., Identification of low-level point radioactive sources using a sensor network. ACM Ttrans. Sensor Network **7**(3), 1–35 (2010). https://doi.org/10.1145/1807048.1807050
21. M.R. Morelande, B. Ristic, Radiological source detection and localisation using Bayesian techniques. IEEE Trans. Signal Proces. **57**(11), 4220–4231 (2009). https://doi.org/10.1109/TSP.2009.2026618
22. J.-C. Chin, D.K. Yau, N.S. Rao, Efficient and robust localization of multiple radiation sources in complex environments, in *IEEE 31st International Conference on Distributed Computing Systems* (2011). https://doi.org/10.1109/ICDCS.2011.94
23. N.S. Rao, S. Sen, N.J. Prins et al., Network algorithms for detection of radiation sources. Nucl. Instrum. Methods A **784**, 326–331 (2015). https://doi.org/10.1016/j.nima.2015.01.037
24. Z. Liu, S. Abbaszadeh, C.J. Sullivan, Spatial-temporal modeling of background radiation using mobile sensor networks. PLoS ONE **13**(10), e0205092 (2018). https://doi.org/10.1371/journal.pone.0205092
25. M. Morelande, B. Ristic, A. Gunatilaka, Detection and parameter estimation of multiple radioactive sources, in *IEEE 10th International Conference on Information Fusion* (2007). https://doi.org/10.1109/ICIF.2007.4408094
26. B. Deb, Iterative estimation of location and trajectory of radioactive sources with a networked system of detectors. IEEE Trans. Nucl. Sci. **60**(2), 1315–1326 (2013). https://doi.org/10.1109/TNS.2013.2247060
27. M. Mitchell, *An Introduction to Genetic Algorithms* (MIT Press, Cambridge, 1998)
28. X.-S. Yang, *Nature-Inspired Metaheuristic Algorithms* (Luniver Press, Bristol, 2010)
29. Y. Shi, Particle swarm optimization: developments, applications and resources, in *IEEE Proceedings of the 2001 Congress on Evolutionary Computation (IEEE Cat. No. 01TH8546)* (2001). https://doi.org/10.1109/CEC.2001.934374
30. M. Dorigo, *Optimization, Learning and Natural Algorithms* (Politecnico di Milano, Milan, 1992)
31. A.E. Ezugwu, J.O. Agushaka, L. Abualigah et al., Prairie dog optimization algorithm. Neural Comput. Appl. **34**(22), 20017–20065 (2022). https://doi.org/10.1007/s00521-022-07530-9
32. J.O. Agushaka, A.E. Ezugwu, L. Abualigah, Gazelle optimization algorithm: a novel nature-inspired metaheuristic optimizer. Neural Comput Appl. **35**, 4099–4131 (2023). https://doi.org/10.1007/s00521-022-07854-6
33. J.O. Agushaka, A.E. Ezugwu, L. Abualigah, Dwarf mongoose optimization algorithm. Comput. Method. Appl. Mech. Eng. **391**, 114570 (2022). https://doi.org/10.1016/j.cma.2022.114570
34. L. Abualigah, M. Abd Elaziz, P. Sumari et al., Reptile Search Algorithm (RSA): a nature-inspired meta-heuristic optimizer. Expert Syst. Appl. **191**, 116158 (2022). https://doi.org/10.1016/j.eswa.2021.116158
35. L. Abualigah, D. Yousri, M. Abd Elaziz et al., Aquila optimizer: a novel meta-heuristic optimization algorithm. Comput. Ind. Eng. **157**, 107250 (2021). https://doi.org/10.1016/j.cie.2021.107250
36. G. Cordone, *Improvements to MLE Algorithm for Localizing Radiation Sources with a Distributed Detector Network* (Clemson University, Clemson, 2019)
37. H.E. Baidoo-Williams, Maximum likelihood localization of radiation sources with unknown source intensity. arXiv:160800427 (2016)
38. G. Cordone, R.R. Brooks, S. Sen et al., Improved multi-resolution method for mle-based localization of radiation sources, in *IEEE 20th International Conference on Information Fusion (Fusion)* (2017). https://doi.org/10.23919/ICIF.2017.8009626
39. S. Arora, S. Singh, The firefly optimization algorithm: convergence analysis and parameter selection. Int. J. Comput. Appl. **69**(3), 48–52 (2013). https://doi.org/10.5120/11826-7528
40. Y. Shi, R. Eberhart, A modified particle swarm optimizer, in *IEEE International Conference on Evolutionary Computation Proceedings* (1998). https://doi.org/10.1109/ICEC.1998.699146
41. A. Engelbrecht, Particle swarm optimization: velocity initialization, in *IEEE Congress on Evolutionary Computation, Brisbane, QLD, Australia* (2012), pp. 1–8. https://doi.org/10.1109/CEC.2012.6256112
42. K. Socha, M. Dorigo, Ant colony optimization for continuous domains. Eur. J. Oper. Res. **185**(3), 1155–1173 (2008). https://doi.org/10.1109/ICNC.2012.6234538
43. S. Pourtakdoust, H. Nobahari, An extension of ant colony to continuous optimization problems, in *Proceedings of the ANTS 2004–Fourth International Workshop on Ant Colony Optimization and Swarm Intelligence* (2004). https://doi.org/10.1007/978-3-540-28646-2_27
44. D. Karaboga, An idea based on honey bee swarm for numerical optimization. Technical report-tr06. Erciyes University (2005)
45. D.A. Cooper, R.J. Ledoux, K. Kamieniecki et al., Intelligent radiation sensor system (irss) advanced technology demonstrator (atd), in *IEEE Conference on Technologies for Homeland Security (HST)* (2012). https://doi.org/10.1109/THS.2012.6459901
46. IRSS "Canonical irss datasets". https://github.com/raonsv/canonical-datasets.
47. J. Klumpp, *Statistical methods for the detection and analysis of radioactive sources* (Colorado State University, Fort Collins, 2014)
48. Y. Shi, R.C. Eberhart, Parameter selection in particle swarm optimization, in *Evolutionary Programming VII International Conference* (1998). https://doi.org/10.1007/BFb0040810